

Optimizing adiabatic quantum pathways via a learning algorithm

Xiaodong Yang,¹ Ran Liu,¹ Jun Li,^{2,*} and Xinhua Peng^{1,3,4,†}

¹*CAS Key Laboratory of Microscale Magnetic Resonance and Department of Modern Physics, University of Science and Technology of China, Hefei, Anhui 230026, China*

²*Shenzhen Institute for Quantum Science and Engineering and Department of Physics, Southern University of Science and Technology, Shenzhen 518055, China*

³*Hefei National Laboratory for Physical Sciences at the Microscale, University of Science and Technology of China, Hefei 230026, China*

⁴*Synergetic Innovation Centre of Quantum Information & Quantum Physics, University of Science and Technology of China, Hefei, Anhui 230026, China*

(Dated: May 30, 2022)

Designing proper time-dependent control fields for slowly varying the system to the ground state that encodes the problem solution is crucial for adiabatic quantum computation. However, inevitable perturbations in real applications demand us to accelerate the evolution so that the adiabatic errors can be prevented from accumulation. Here, by treating this trade-off task as a multi-objective optimization problem, we propose a gradient-free learning algorithm with pulse smoothing technique to search optimal adiabatic quantum pathways and apply it for Landau-Zener Hamiltonian and Grover search Hamiltonian. Numerical comparisons with linear schedule, local adiabatic theorem induced schedule and a gradient-based algorithm searched schedule reveal that the proposed method can achieve significant performance improvements in terms of the adiabatic time and the instantaneous ground state population maintain. The proposed method can be used to solve more complex and real adiabatic quantum computation problems.

I. INTRODUCTION

Adiabatic quantum computation (AQC) [1], which is known to be polynomially equivalent [2] to the standard circuit-based quantum computation, offers us an alternative way to solve many challenging optimization problems, such as traveling salesman problem [3] and satisfiability problem [4]. It functions by designing a target Hamiltonian whose ground state encodes the solution of the optimization problem of interest, and slowly evolving the system to this target Hamiltonian from some simple initial Hamiltonian whose ground state can be easily prepared. According to the quantum adiabatic theorem [4, 5], so long as the system evolves sufficiently slowly and the external uncertainties have only negligible effects on the system, the final state of the system will be the ground state of the target Hamiltonian, as expected.

In actual applications, though AQC has inherent robustness to some sources of noises, such as dephasing and unitary control errors [6, 7], its effectiveness could still be severely hampered by other inevitable perturbations. Consequently, many error suppression and error correction methods [8–11] have been developed to handle this problem. However, recent study [10] shows that these methods are not sufficiently fault-tolerant, and they are rather resource-consuming. A more practical and direct approach is to design a sufficient fast adiabatic evolution path, for the sake of reducing the accumulations of the adiabatic errors.

Shortcuts to adiabaticity [12] is a representative approach to accelerate the transition to the target state, but it always needs complicated analytical derivations, detailed information of instantaneous adiabatic state of the system, or unfeasible additional terms [13]. Furthermore, it inherently can not maintain the instantaneous ground state during the evolution process, thus not proper for most of the AQC applications. Recent efforts have brought new opportunities to adiabatically accelerate the evolution by optimal control methods, including analytical quantum adiabatic brachistochrone (QAB)[14], numerical Lyapunov control [15] and gradient-based methods [16, 17]. However, QAB is only suitable for low dimensional parameterizations and does not consider the population loss during the evolution process. Gradient-based methods greatly rely on initial trial controls, their derivates cost abundant resource to obtain, and they are more easily trapped into the local extremes for complex optimization problems [18].

Here, we formulate this task, i.e., decreasing the adiabatic time while minimizing the population loss from the instantaneous ground state, as a multi-objective optimization problem. We employ a simple but powerful differential evolution (DE) [19–21] algorithm to explore the tradeoffs between these two objectives. Such gradient-free learning algorithms have drawn much attention in recent studies for their ability in producing high-quality controls and designing better experiments [22–29]. In this study, specifically, we consider cases where all the controls in the time-dependent Hamiltonian can vary freely but with amplitude constraints and the objective function to be maximized contains two weighted terms: the target state fidelity and the averaged system energy during the evolution. These multi-objective optimization

*Electronic address: lij3@sustech.edu.cn

†Electronic address: xhpeng@ustc.edu.cn

problems with constraints are very hard to solve analytically. Compared to a recent work using gradient-based algorithm (called D-MORPH) and instantaneous ground state tracking [16] to solve this multi-objective problem, our approach promises larger probability in finding global optimal solutions and is more practical to iteratively implement in real experiments. As illustrative applications, we perform numerical demonstrations on Landau-Zener Hamiltonian [30] and Grover search Hamiltonian [31] using the proposed approach. Comparisons are also made to show the advantages of our approach over the above mentioned gradient-based method. Further practical and complex applications of our method for AQC computation are also briefly discussed.

The remainder of the paper is organized as follows. We first introduce the AQC basics and formulate the pathway optimization problem in a general setting in Section II. The learning algorithm for AQC is then described in Section III. Afterwards, we choose two representative pathway optimization problems and compare the numerical simulation results of our proposed method and some previously reported methods in literature in Section IV. Finally, in Section V, some brief conclusions and discussions are presented.

II. BACKGROUNDS AND PROBLEM SETUP

Consider an n -qubit quantum system which evolves under the following Schrödinger equation ($\hbar = 1$):

$$\frac{d|\psi(t)\rangle}{dt} = -i\mathcal{H}(t)|\psi(t)\rangle, \quad t \in [0, T], \quad (1)$$

where $\mathcal{H}(t)$ represents the time-dependent system Hamiltonian and the Hilbert space dimension is $N = 2^n$. Thus, the quantum state $|\psi(t)\rangle$ can be transformed with $|\psi(t)\rangle = U(t)|\psi(0)\rangle$, where the evolution operator $U(t)$ satisfies $dU(t)/dt = -i\mathcal{H}(t)U(t)$, $U(0) = I$. The instantaneous eigenstates and eigenenergies of $\mathcal{H}(t)$ can then be defined by

$$\mathcal{H}(t)|\phi_m(t)\rangle = E_m(t)|\phi_m(t)\rangle \quad (2)$$

with $m = 0, 1, \dots, N-1$ and $E_0(t) \leq E_1(t) \leq \dots \leq E_{N-1}(t)$. Here, we mainly concern the energy gap between the ground state and the first excited state, i.e., $g(t) = E_1(t) - E_0(t)$.

To perform AQC, the routine is to first prepare the system at the ground state $|\psi(0)\rangle = |\phi_0(0)\rangle$ of the initial Hamiltonian $\mathcal{H}_I = \mathcal{H}(0)$, which is assumed to be easily prepared. The system then evolves slowly under the constructed Hamiltonian

$$\mathcal{H}(t) = \mathcal{H}[\mathbf{u}(t)] = u_1(t)\mathcal{H}_I + u_2(t)\mathcal{H}_P, \quad (3)$$

where $\mathcal{H}_P = \mathcal{H}(T)$ represents the problem Hamiltonian, $u_1(t), u_2(t)$ are control fields satisfying the boundary conditions $u_1(0) = u_2(T) = 1$, $u_1(T) = u_2(0) = 0$ and amplitude constraints $0 \leq u_l(t) \leq 1$, $l = 1, 2$. As designed,

the ground state $|\phi_0(T)\rangle$ of \mathcal{H}_P encodes the solution to the computational problem. The quantum adiabatic theorem [4, 5] guarantees that so long as the evolution is sufficiently slow and the external perturbations can be ignored, the system's final state $|\psi(T)\rangle$ will be the target ground state $|\phi_0(T)\rangle$. To quantify their distance, we define the state fidelity $F_1 = |\langle\phi_0(T)|\psi(T)\rangle|^2$.

The control schedules $\mathbf{u}(t) = (u_1(t), u_2(t))$ that dominates the above system evolution, which we called adiabatic quantum pathways, are very crucial for the reliable realization of AQC. Different methods have been developed to design or search such controls, as mentioned before. For the following comparisons with our proposed method, here we briefly review two conventional methods. The first one is to use linear interpolation control fields [32] (marked as Linear), i.e., $u_2(s) = 1 - u_1(s) = s$, where we use the rescaled time $s = t/T$. Another one is based on local adiabatic evolution theorem [1, 32] (RC for short), for Grover search Hamiltonian, it's $u_2(s) = 1 - u_1(s) = 1/2 + \tan[(2s-1)\tan^{-1}\sqrt{N-1}/2\sqrt{N-1}]$ with $s = t/T$.

III. DIFFERENTIAL EVOLUTION ALGORITHM FOR AQC

To numerically optimize the control schedules using the differential evolution algorithm, we should first set a performance function to evaluate these controls. As mentioned previously, we use a multi-objective function as follows [16]

$$F = |\langle\phi_0(T)|\psi(T)\rangle|^2 - \frac{\alpha}{T} \int_0^T \langle\psi(t)|\mathcal{H}(t)|\psi(t)\rangle dt, \quad (4)$$

where $\alpha > 0$ is a positive weight factor that determines the relative importance of the first term (F_1), which represents the main physical goal, and the second term (with minus, denoted as F_2), which is used to minimize the population loss from the instantaneous ground state during the evolution. Additionally, to quantify the instantaneous population loss, we define the instantaneous ground state population $P_0(t) = |\langle\phi_0(t)|\psi(t)\rangle|^2$.

The optimal control schedules should not only maximize the above multi-objective function but also be smooth enough so that the real applications can realize predicted performance. To achieve this, we use the chopped random basis (CRAB) technique [33] to express the controls to-be-optimized in a set of truncated Fourier basis

$$u_l(s) = u_l^g(s)\{1 + \sum_{k=1}^{N_c} [a_l^k \sin(\omega_l^k s) + b_l^k \cos(\omega_l^k s)]\}, \quad (5)$$

where we use the scaled time $s = t/T$, $l = 1, 2$ indicate the index of the two control fields, $u_l^g(s)$ represents the initial controls guess. Thus, the optimization of the control schedules $\mathbf{u}(s) = (u_1(s), u_2(s))$ is to search

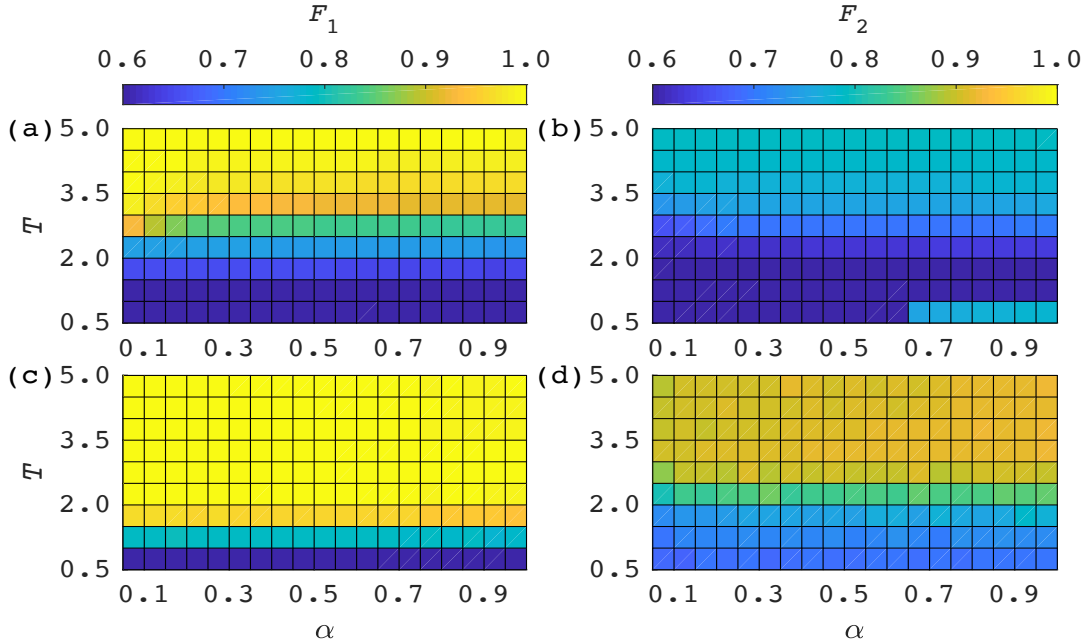


FIG. 1: (Color online) Performance function values F_1 and F_2 versus different combinations of the adiabatic time T and the weight factor α for Landau-Zener Hamiltonian. (a) and (b) plot the averaged results obtained by D-MORPH over 5 runs. The maximum iteration number was $G_{\max} = 1000$. The stepsize λ^G was initialized as 0.02 and decreased with a factor 0.5 if the calculated F was worse than the previous one but with the maximum trial times 100. The control fields were all bounded in the range $[0, 1]$ during the optimization. (c) and (d) plot the averaged results produced by DE over 5 runs. The maximum iteration number was $G_{\max} = 300$, and the initial guess was chosen as $u_1^g(s) = 1 - s, u_2^g(s) = s$. The algorithm parameters were: $S = 0.6, C = 0.95, P = 20, D = 12, N_c = 2$. Moreover, the controls were also constrained in the range $[0, 1]$ during the searching process.

$6N_c$ optimal parameters $X = (a_1^k, b_1^k, \omega_1^k, a_2^k, b_2^k, \omega_2^k)$ ($k = 1, 2, \dots, N_c$) that maximize the above performance function Eq. 4. In addition, to perform amplitude constraints on the control fields, we use the unity-based normalization, i.e., $u_l(s) = (u_l(s) - u_l^{\min}) / (u_l^{\max} - u_l^{\min})$, where u_l^{\max} and u_l^{\min} represent the maximum amplitude and the minimum amplitude of $u_l(s) : s \in [0, 1]$, respectively.

Differential evolution algorithm [19–21], as a simple but competitive real-valued gradient-free optimization method, is applied here to optimize these parameters. It functions by simulating the natural evolution process through applying the steps of operators mutation, crossover and selection in the population space which is made up of a set of individuals. The detailed algorithm procedures are described as follows.

Step 1: Set the algorithm parameters: scaling factor S , crossover rate C , chromosome length (the dimension of each individual) D and population size P . Generate an initial population $Pop = \{X_1^0, \dots, X_P^0\}$ randomly, with $X_i^0 = [X_{i1}^0, \dots, X_{iD}^0]$ being the i -th individual in current population.

Step 2: Update the iteration number $G = G + 1$, and from $i = 1$ to P , do the following steps:

(1) **Mutation.** Generate a donor vector $V_i^G = [V_{i1}^G, \dots, V_{iD}^G]$ through the differential mutation scheme of DE: $V_i^G = X_{r_b^i}^{G-1} + S \cdot (X_{r_1^i}^{G-1} - X_{r_2^i}^{G-1}) + S \cdot (X_{r_3^i}^{G-1} -$

$X_{r_4^i}^{G-1})$, where $r_1^i, r_2^i, r_3^i, r_4^i$ are randomly chosen mutually exclusive integers in the range $[0, P]$ and r_b^i is the index of the best individual in current population.

(2) **Crossover.** Generate a trial vector $U_i^G = [U_{i1}^G, \dots, U_{iD}^G]$ by binomial crossover strategy: if $rand_{i,j}[0, 1] \leq C$ or $j = j_{rand}$, let $U_{ij}^G = V_{ij}^G$, where $j_{rand} \in [1, 2, \dots, D]$ is a randomly chosen index. Otherwise let $U_{ij}^G = X_{ij}^{G-1}$.

(3) **Selection.** Evaluate the former individual X_i^{G-1} and the trial vector U_i^G , if $f(U_i^G) \leq f(X_i^{G-1})$, let $X_i^G = U_i^G$, otherwise keep $X_i^G = X_i^{G-1}$ unchanged.

Step 3: Check the stopping criterion, if not satisfied, go to *Step 2*.

We will also compare our method with the recent presented gradient-based D-MORPH [16] method. In D-MORPH, the new controls can be refreshed iteratively by

$$u_l^{G+1}(t) = u_l^G(t) + \lambda^G \partial F / \partial u_l^G(t) \quad (6)$$

until the stopping criterion is met, where λ^G is some appropriate stepsize, $\partial F / \partial u_l^G(t)$ is the functional derivative of the objective with respect to each control field.

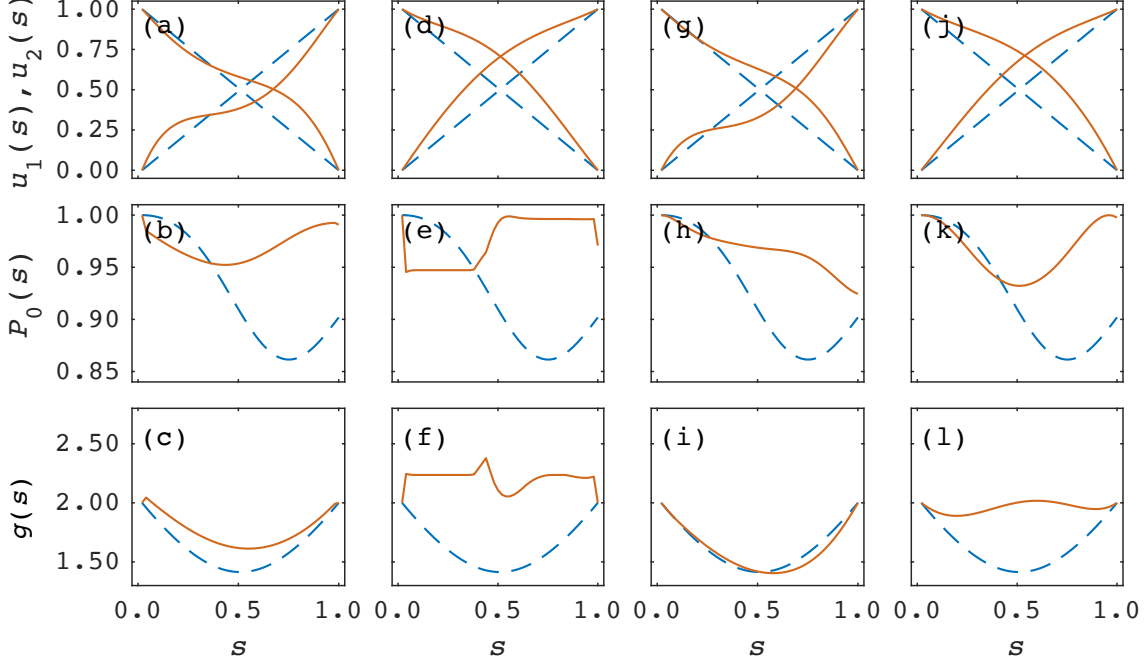


FIG. 2: (Color online) Optimization results for Landau-Zener Hamiltonian obtained by the method Linear, D-MORPH and DE. The controls fields $u_1(s)$ and $u_2(s)$, the instantaneous ground-state population $P_0(s)$ and the energy gap $g(s)$ are shown versus the scaled time s optimized by (a)–(c) D-MORPH (solid red line) and Linear (dashed blue line) when $T = 3, \alpha = 0.1$; (d)–(f) DE (solid red line) and Linear (dashed blue line) when $T = 3, \alpha = 0.1$; (g)–(i) D-MORPH (solid red line) and Linear (dashed blue line) when $T = 3, \alpha = 0.5$; (j)–(l) DE (solid red line) and Linear (dashed blue line) when $T = 3, \alpha = 0.5$.

IV. APPLICATIONS

To show the advantages of our proposed method, we chose two representative examples, i.e., Landau-Zener type Hamiltonian [30] and Grover search algorithm type Hamiltonian [31], to demonstrate the numerical simulations.

1. Landau-Zener Hamiltonian

As a simple but nontrivial start-up, we explored the adiabatic quantum pathways of Landau-Zener Hamiltonian $\mathcal{H}_I = \sigma_z, \mathcal{H}_P = \sigma_x$, where σ_x and σ_z are Pauli matrices. Adiabatic time T is crucial for the realization of AQC, it should be set carefully so that the system can evolve sufficiently slowly but without accumulating too many adiabatic errors. Moreover, as we use a multi-objective function to adjust the control schedules for optimal adiabatic quantum pathways, the weight factor α is very important for the success of the optimization.

Therefore, we first studied the performance function values F_1 and F_2 with respect to different combinations of T and α for the method D-MORPH and DE, as shown in Fig. 1. Here, sufficiently large iteration number was set for both of the methods so that the best performance function values could be reached in each case with the settled T and α . From the comparison between Fig.

1(a) and Fig. 1(c), a direct and general conclusion is that DE performs better than D-MORPH for realizing the main physical goal, i.e., DE results in a final state closer to the ground state of the problem Hamiltonian. More detailedly, we find that when T is greater than 3, D-MORPH has a comparable performance with DE for most of the weight factor α . However, when T is smaller than 3, DE can still achieve a very high state fidelity F_1 for most of the cases but D-MORPH fails. What's more, if we focus on the issue that how the weight factor α affects on F_1 , we can see that the performance of D-MORPH is much more sensitive to the choice of α than that for DE, and smaller α is more likely to achieve better performance for D-MORPH. Besides maximizing the main goal F_1 , we also care about minimizing the population loss during the optimization process. The comparisons in Fig. 1(b) and Fig. 1(d) reveal that DE performs better than D-MORPH also for optimizing F_2 , especially for large adiabatic times and small weight factors. These results in Fig. 1 indicate that when searching optimal adiabatic quantum pathways for Landau-Zener Hamiltonian, DE has great advantages over D-MORPH for a wide range of parameters T and α . To make this more concrete, we quantitatively compare these two methods and show some typical results in Table I.

In the following, from the above simulations we chose two sets of the combinations of T and α to demonstrate the controls fields, the instantaneous ground-state popu-

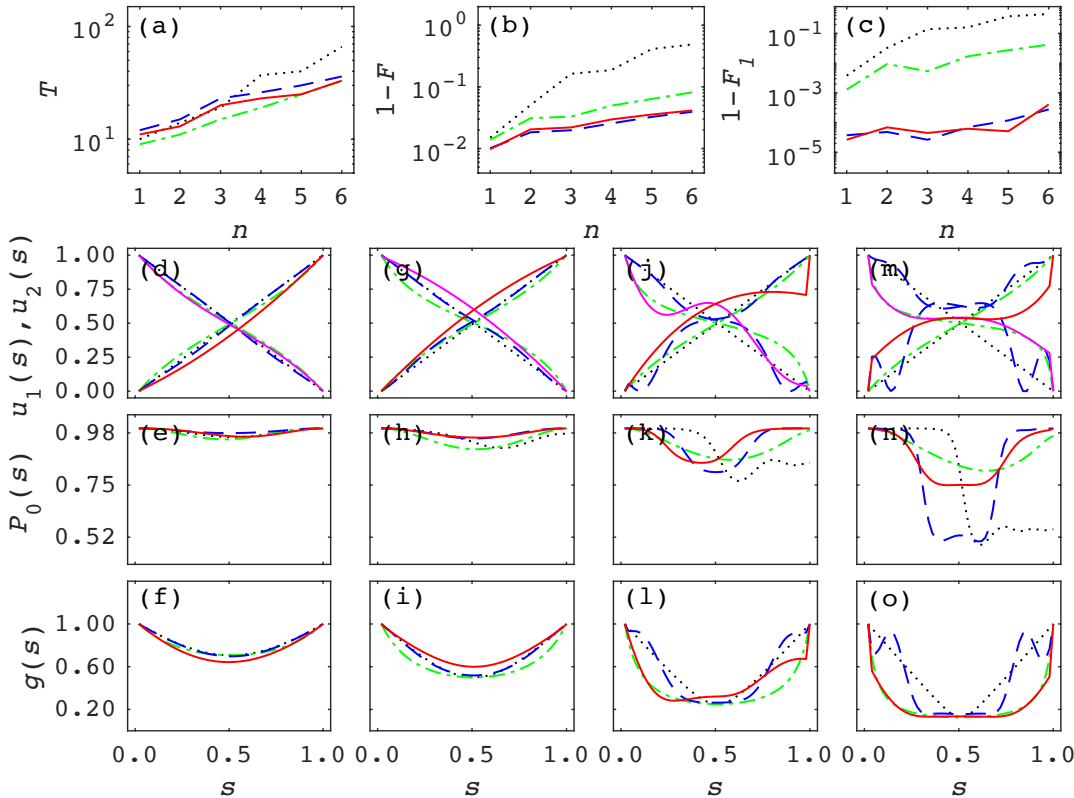


FIG. 3: (Color online) Optimization results for Grover search algorithm Hamiltonian using $n = 1$ to 6 qubits obtained by the methods Linear, RC, D-MORPH and DE. (a) plots the searched minimum adiabatic time T versus the qubit number n when $\alpha = 0.1$, where T was gradually increased and stopped when the difference between two successive F was smaller than 10^{-3} . (b) and (c) plot the corresponding searched final performance function values $1 - F$ and $1 - F_1$ versus n . The control fields $u_1(s)$ and $u_2(s)$, the instantaneous ground-state population $P_0(s)$ and the energy gap $g(s)$ are shown versus the scaled time s for (d)–(f) $n = 1$; (g)–(i) $n = 2$; (j)–(l) $n = 4$; (m)–(o) $n = 6$. In all figures, the different methods are Linear (dotted black line), RC (dash-dotted green line), D-MORPH (dashed blue line), DE (solid red line), and all the algorithm parameters were the same as the above Landau-Zener Hamiltonian case.

α	D-MORPH			DE		
	F_1	F_2	F	F_1	F_2	F
0.05	0.9856	0.7352	1.0224	0.9999	0.9093	1.0451
0.1	0.9680	0.7433	1.0423	0.9997	0.9036	1.0901
0.2	0.9460	0.7519	1.0964	0.9992	0.9071	1.1806
0.4	0.9287	0.7534	1.2300	0.9980	0.9132	1.3633
0.6	0.9210	0.7541	1.3735	0.9963	0.9161	1.5460
0.8	0.9159	0.7555	1.5203	0.9958	0.9150	1.7278
1.0	0.9119	0.7568	1.6688	0.9938	0.9193	1.9131

TABLE I: Optimization results searched by D-MORPH and DE for Landau-Zener Hamiltonian. The target state fidelity (F_1) and the averaged system energy during the evolution (F_2) are shown with different weight factors α . The adiabatic time was all chosen as $T = 3$.

lation and the energy gap obtained by the method Linear, D-MORPH and DE, as shown in Fig. 2. By comparing the instantaneous ground-state population in Fig. 2(b),(h) for D-MORPH and that in Fig. 2(e),(k) for DE, we find that during the evolution DE has generally

smaller population loss when $\alpha = 0.1$ and $\alpha = 0.5$, and both of them beat the method Linear. Moreover, from the comparison of Fig. 2(c),(i) and 2(f),(l), we find that energy gap induced by DE is almost the inverse of that induced by Linear for both cases $\alpha = 0.1$ and 0.5 , and it can be greater than 2 at all times during the evolution when $\alpha = 0.1$. However, the energy gap induced by D-MORPH is similar to that of Linear when $\alpha = 0.1$ and $\alpha = 0.5$. These results indicate that the improved performance is achieved by a gap increment at intermediate times.

2. Grover Search Algorithm Hamiltonian

We also considered a more practical and complex example, namely Grover search algorithm, which is used to identify a marked element in an unsorted database of N elements. Precisely speaking, its Hamiltonian can be denoted as $\mathcal{H}_I = \mathcal{I} - |\varphi\rangle\langle\varphi|$, $\mathcal{H}_P = \mathcal{I} - |m\rangle\langle m|$, where \mathcal{I} is the identity matrix, $|\varphi\rangle$ is the uniform superposition

state $|\varphi\rangle = \sum_{i=0}^{N-1} |i\rangle / \sqrt{N}$, $\{|i\rangle\}$ are the basis states of the Hilbert space and $|m\rangle$ is the marked state. Local adiabatic evolution theorem [32] based RC promises an adiabatic time of order \sqrt{N} , which is a quadratic speed-up compared to the classical method Linear. Optimization algorithms D-MORPH and DE are expected to surpass or at least be close to this scaling.

Thus, we first explored the minimum adiabatic time T needed to reach a sufficiently high F versus the number of qubits n for these methods, the results are shown in Fig. 3(a). One can find that D-MORPH, DE and RC all have a quadratic speed-up than Linear, as expected. Moreover, the adiabatic time needed for DE is always smaller than that for D-MORPH, which indicates that DE can achieve faster adiabatic evolution than D-MORPH. To show the corresponding performance function values F and F_1 obtained by these methods, we plot Fig. 3(b) and Fig. 3(c), from which we find that DE achieves a comparable multi-objective function value F with D-MORPH. For the state fidelity F_1 , DE also has comparable performance with D-MORPH for most of the cases.

We then proceed by demonstrating the control fields, the instantaneous ground-state population and the energy gap obtained by these methods for the number of qubits $n = 1, 2, 4, 6$, as shown in the rest parts of Fig. 3. The instantaneous ground-state population comparisons plotted in Fig. 3(e),(h),(k),(n) reveal that DE performs much better for reducing the population loss during the evolution compared to D-MORPH, especially for large number of qubits, i.e., $n = 4, 6$. The corresponding energy gap comparisons shown in Fig. 3(f),(i),(l),(o) report generally similar behaviors of all the methods, suggesting that we may need more careful research on adjusting the energy gaps by the searched optimal control schedules to further improve the adiabatic quantum pathways. By exploring the adiabatic pathways of Grover search algorithm Hamiltonian by Linear, RC, D-MORPH and DE, we can conclude that DE achieves almost fastest adiabatic evolution, while achieving the least instantaneous ground state population loss.

In addition, we briefly analyze the computational costs of D-MORPH and DE in searching optimal control schedules here. They are partly determined by the algorithm parameters, including S, C, P, D, N_c for DE and λ^G for D-MORPH, which are very important for the performance of the algorithms. However, a thorough tuning of the parameters will be a resource-consuming and unrealistic task. For our simulations, S, C, P are chosen from our experiences and $D, N_c, \lambda^G, G_{\max}$ are settled by sufficient trials. In this way, we expect that D-MORPH and DE perform possibly close to their best status, respectively. We then show the run time per iteration and the total run time for these two methods in Fig. 4, where we find that DE needs significantly more run time per iteration than that for D-MORPH. However, the total run time for DE is a little longer than that for D-MORPH when the number of qubits $n = 1 \sim 5$, and shorter when $n = 6$. From these analysis, we can roughly conclude that the

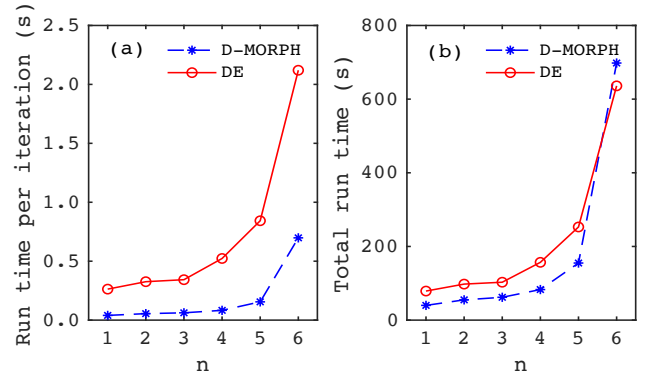


FIG. 4: (Color online) Run time of D-MORPH and DE for Grover search algorithm Hamiltonian. (a) plots the run time per iteration with respect to the number of qubits n , and (b) shows the total run time regarding the number of qubits n .

computational costs of the two methods are comparable and both in an acceptable range.

V. CONCLUSIONS AND DISCUSSIONS

In this study, for the first time, we have proposed a differential evolution algorithm with CRAB technique to explore the optimal adiabatic quantum pathways for AQC and apply it to Landau-Zener Hamiltonian and Grover search algorithm Hamiltonian. This gradient-free learning algorithm performs better than conventional methods including Linear and RC that are based on adiabatic theorems. This is because that most of the adiabatic theorems are not exact so that their induced adiabatic pathways are approximate. Even these conventional approaches can give nearly optimal solutions, a more easy-to-implement numerical method will be more friendly to applications. Moreover, compared to a recent gradient-based D-MORPH method, our method also has advantages in terms of realizing high-fidelity target ground state with shorter adiabatic time and reducing the population loss from the instantaneous ground state. The merits of our gradient-free method mainly come from two reasons [18]: (1) For multi-objective optimization problems, the landscape of the performance function usually contains many local extrema. Gradient-based algorithms start from one trial point and move along the derivative direction, thus are very likely to get trapped in these local extrema. However, evolutionary-based algorithms start from a group of points distributed in the whole parameter space and update according to some evolutionary rules, thus having more chance to escape from these local extrema and reach the global optima. (2) The to-be-optimized adiabatic quantum pathways contain amplitude constraints (in the range $[0, 1]$), this greatly influences the performance of the optimization algorithms and also induces local extrema [34]. For gradient-based type, the amplitudes of the control

fields vary depending on the continuous derivate functions, thus the amplitude constraints will very likely induce the convergence to the false extreme. However, for gradient-free algorithms, the amplitudes change with more degrees of freedom, they can be finely tuned to reach the true global optima.

This numerical optimization method can handle multi-objective and constraints more easily, the complexity of the searching procedures for the optimal pathways does not increase much for more complex problems, thus is more practical and useful for applied AQC. The successful applications here encourage us to extend it to more complicated AQC optimization tasks, such as satisfiability problems [4], random optimization problems [35]. Moreover, the proposed method can become an important tool for developing current quantum annealing hardware and future AQC processors, such as D-Wave systems [36].

Moreover, in real applications, analytical or numerical designed adiabatic quantum pathways may not behave as expected due to inevitable perturbations. However, our method can be easily adapted to closed-loop type to handle these perturbations. The reasons are the performance function chosen here can be efficiently measured

and the learning algorithm is resource-saving compared to those gradient-based types.

ACKNOWLEDGEMENTS

X. P. is supported by National Key Research and Development Program of China (Grant No. 2018YFA0306600), the National Science Fund for Distinguished Young Scholars (Grant No. 11425523), Projects of International Cooperation and Exchanges NSFC (Grant No. 11661161018), Anhui Initiative in Quantum Information Technologies (Grant No. AHY050000). J. L. is supported by the National Natural Science Foundation of China (Grants No. 11975117, No. 11605005, No. 11875159, and No. U1801661), Science, Technology and Innovation Commission of Shenzhen Municipality (Grants No. ZDSYS20170303165926217, No. JCYJ20170412152620376, and No. JCYJ20180302174036418)), Guangdong Innovative and Entrepreneurial Research Team Program (Grant No. 2016ZT06D348).

[1] T. Albash and D. A. Lidar, *Rev. Mod. Phys.* **90**, 015002 (2018).

[2] D. Aharonov, W. Van Dam, J. Kempe, Z. Landau, S. Lloyd, and O. Regev, *SIAM Rev.* **50**, 755 (2008).

[3] R. Martoňák, G. E. Santoro, and E. Tosatti, *Phys. Rev. E* **70**, 057701 (2004).

[4] E. Farhi, J. Goldstone, S. Gutmann, J. Lapan, A. Lundgren, and D. Preda, *Science* **292**, 472 (2001).

[5] E. Farhi, J. Goldstone, S. Gutmann, and M. Sipser, *arXiv:0001106* (2000).

[6] A. M. Childs, E. Farhi, and J. Preskill, *Phys. Rev. A* **65**, 012322 (2001).

[7] M. H. S. Amin, D. V. Averin, and J. A. Nesteroff, *Phys. Rev. A* **79**, 022107 (2009).

[8] S. P. Jordan, E. Farhi, and P. W. Shor, *Phys. Rev. A* **74**, 052322 (2006).

[9] D. A. Lidar, *Phys. Rev. Lett.* **100**, 160506 (2008).

[10] K. C. Young, M. Sarovar, and R. Blume-Kohout, *Phys. Rev. X* **3**, 041013 (2013).

[11] M. Sarovar and K. C. Young, *New J. Phys.* **15**, 125032 (2013).

[12] D. Guéry-Odelin, A. Ruschhaupt, A. Kiely, E. Torrontegui, S. Martínez-Garaot, and J. G. Muga, *Rev. Mod. Phys.* **91**, 045001 (2019).

[13] K. Takahashi, *J. Phys. Soc. Jpn.* **88**, 061002 (2019).

[14] A. T. Rezakhani, W.-J. Kuo, A. Hamma, D. A. Lidar, and P. Zanardi, *Phys. Rev. Lett.* **103**, 080502 (2009).

[15] W. Wang, S. Hou, and X. Yi, *Ann. Phys.* **327**, 1293 (2012).

[16] C. Brif, M. D. Grace, M. Sarovar, and K. C. Young, *New J. Phys.* **16**, 065013 (2014).

[17] G. Quiroz, *Phys. Rev. A* **99**, 062306 (2019).

[18] K. Price, R. M. Storn, and J. A. Lampinen, *Differential evolution: a practical approach to global optimization* (Springer Science & Business Media, 2006).

[19] R. Storn and K. Price, *J. Global Optim.* **11**, 341 (1997).

[20] S. Das and P. N. Suganthan, *IEEE Trans. Evol. Comput.* **15**, 4 (2011).

[21] S. Das, S. S. Mullick, and P. N. Suganthan, *Swarm Evol. Comput.* **27**, 1 (2016).

[22] R. S. Judson and H. Rabitz, *Phys. Rev. Lett.* **68**, 1500 (1992).

[23] C. Brif, R. Chakrabarti, and H. Rabitz, *New J. Phys.* **12**, 075008 (2010).

[24] R. Rey-de Castro, Z. Leghtas, and H. Rabitz, *Phys. Rev. Lett.* **110**, 223601 (2013).

[25] E. Zahedinejad, J. Ghosh, and B. C. Sanders, *Phys. Rev. Lett.* **114**, 200502 (2015).

[26] E. Zahedinejad, J. Ghosh, and B. C. Sanders, *Phys. Rev. Applied* **6**, 054005 (2016).

[27] M. Krenn, M. Malik, R. Fickler, R. Lapkiewicz, and A. Zeilinger, *Phys. Rev. Lett.* **116**, 090405 (2016).

[28] F. Frank, T. Unden, J. Zoller, R. S. Said, T. Calarco, S. Montangero, B. Naydenov, and F. Jelezko, *npj Quantum Inf.* **3**, 48 (2017).

[29] X. Yang, J. Li, and X. Peng, *Sci. Bull.* **64**, 1402 (2019).

[30] M. G. Bason, M. Viteau, N. Malossi, P. Huillery, E. Arimondo, D. Ciampini, R. Fazio, V. Giovannetti, R. Manella, and O. Morsch, *Nat. Phys.* **8**, 147 (2012).

[31] L. K. Grover, *Phys. Rev. Lett.* **79**, 325 (1997).

[32] J. Roland and N. J. Cerf, *Phys. Rev. A* **65**, 042308 (2002).

[33] T. Caneva, T. Calarco, and S. Montangero, *Phys. Rev. A* **84**, 022326 (2011).

[34] K. W. Moore and H. Rabitz, *J. Chem. Phys.* **137**, 134113 (2012).

[35] V. Bapst, L. Foini, F. Krzakala, G. Semerjian, and

F. Zamponi, [Phys. Rep. **523**, 127 \(2013\)](#).

[36] M. W. Johnson, M. H. Amin, S. Gildert, T. Lanting, F. Hamze, N. Dickson, R. Harris, A. J. Berkley, J. Johansson, P. Bunyk, *et al.*, [Nature **473**, 194 \(2011\)](#).